Desalination and Water Treatment
www.deswater.com

doi:10.5004/dwt.2019.23974

156 (2019) 87–95
July

Single and binary sorption of reactive dyes onto red seaweed-derived biochar: multi-component isotherm and modelling

J. Thivya[a,*], J. Vijayaraghavan[b]

[b]Department of Civil Engineering, University College of Engineering Dindigul, Dindigul 624 622, Tamil Nadu, India, Tel: +91 94426 45058, email: thivyame@gmail.com (J. Thivya)
[b]Department of Civil Engineering, University College of Engineering Ramanathapuram, Ramanathapuram 623513, Tamil Nadu, India, Tel: +91-9488528279, email:vijayaraghavanmalar@gmail.com (J. Vijayaraghavan)

Received 28 September 2018; Accepted 17 February 2019

ABSTRACT

The ability of *Kappaphycus alvarezii*-derived biochar (KAB) to adsorb Reactive blue 4 (RB4) and Reactive orange 16 (RO16) in mono- and binary contaminated waters have been investigated. KAB, produced at 350°C and 2 h through pyrolysis, exhibited dye sorption capacities 3.1 times higher than raw *K. alverzii*. The surface of biochar was analysed through FT-IR and SEM results. The pH edge experimental trails indicated that electrostatic attraction between biochar surface and reactive dye anions was favoured under acidic conditions. Biosorption isotherm experiments revealed that in mono-dye solutions, KAB excelled in RB4 sorption with highest experimental uptake of 0.324 mmol/g, compared to RO16 uptake of 0.140 mmol/g. In binary solutions, RO16 sorption capacity of KAB was inhibited by 68.5% in the presence of RB4; whereas RB4sorption capacity was slightly better. This inhibition effect is due to combination of several factors, and the crucial factor being the reactivity of the two dyes. Mono and binary Freundlich and Langmuir equations successfully described the single and binary RB4-RO16 sorption isotherms with high accuracy.

Keywords: Multi-component solutions; Competitive adsorption; Dye effluents; Dye competition; Biochar

1. Introduction

Dye remediation from factory/industry effluents is recognized as a challenge in wastewater treatment/management scheme because of their complex chemical composition and extreme physicochemical conditions, which pose severe problems even for well-established remediation methods. Industries such as paper, plastic, leather, textile and ink manufacturing utilize large quantities of dyes and thus the wastewater generated often contain dye residues. One important and extensively used dye group is reactive dye. In general, reactive dyes are azo-based chromophores constitute of different reactive groups. Owing to their favourable features such as water-fastness, bright color along with simple application methods, reactive dyes are very popular in textile industries [1]. Nevertheless, during dyeing of cellulose fibres approximately 50% of reactive dyes may be lost to the wastewaters. Due to their complex nature, reactive dyes are difficult to treat through traditional effluent treatment methods [2]. For instance, Pierce [3] indicated that approximately 90% of reactive dyes remain in the treated solution after employing activated sludge treatment process. Hence, development of effective methods/processes to remediate reactive dye-bearing effluents is on the horizon.

Several methods have been developed and subsequently employed for reactive dye removal, such as membrane filtration, oxidation process, ion-exchange process, electrochemical technology, photocatalytic degradation and adsorption [4–8]. Of these methods, adsorption is often demonstrated as effective remediation method for dye-bearing wastewaters [9–11]. However, some of the efficient adsorbent is often expensive such as activated car-

---

*Corresponding author.

bon. Hence search for cheap, environmentally-benign and efficient sorbents for dye-containing effluents is the most researched subject in recent years. Seaweeds are efficient and well-established adsorbents for heavy metals [12]; however they often exhibit mediocre performance towards reactive dyes [13] owing to the presence of excess negatively charged binding groups. Hence, attempts were made in this study to prepare biochar from seaweed biomass and subsequently examine the potential of seaweed-derived biochar to remove reactive dyes.

The adsorption of single-component dye systems using various sorbents is a reasonably well researched field [9,14], however it should be noted that effluents emanating from industries generally comprises of several dyes. In this scenario, sorption becomes competitive in which one dye competes with other in occupying the functional groups/pores of the sorbent. Few researchers attempted dye removal from multi-dye solutions [15,16]; however the competition between two dyes, removal mechanism and competitive modelling has not fully understood. In the field of adsorption, the understanding and predication of multi-solute sorption equilibrium is still very challenging [17]. For instance, adsorption of specific dye from multi-solute systems may lead to uneven concentration spikes and overshoot of specific contaminant due to competition between solutes. Thus, the aim of this research is to study the mono and binary sorption of Reactive blue 4 and Reactive orange 16 using seaweed-derived biochar. To achieve this goal, we used *Kappaphycus alvarezii* as feed stock for preparation of biochar.

2. Materials and methods

2.1. Seaweed biochar and reactive dyes

Kappaphycus alvarezii biomass was collected from Mandapam, a coastal area of Tamil Nadu, India. The collected seaweeds were rinsed with distilled water and subsequently exposed to natural drying. The dried biomass was grounded to coarse powder and sieved to achieve particles of 0.75 mm. A known quantity (100 g) of dried seaweed sample was placed in a covered crucible (aluminium foil with two small vents) and heated in an electrical muffle furnace to 350°C and maintained at the same condition for 2 h [18]. The muffle furnace was initially purged with N_2 to provide a low-oxygen environment. After pyrolysis, the furnace is allowed to cool down and once the temperature inside the furnace reached that of room temperature, the biochar was taken out of the furnace. It was kept in a desiccator and subsequently employed for sorption studies.

Reactive blue 4 (RB4) and Reactive orange 16 (RO16) were obtained from Sigma-Aldrich India. Table 1 lists the chemical structures of two reactive dyes along with other characteristics. The concentration of reactive dyes were analysed using a spectrophotometer (Merck, Spectroquant-Phara 300). In the case of mono-dye systems, the concentration of RB4 and RO16 was estimated by quantifying the absorbance at 595 and 494 nm, respectively. In a binary system, RB4 and RO16 concentrations were measured using the below equation [19]:

$$C_{RB4} = (K_{RO162}d_{RB4} - K_{RO161}d_{RO16})/(K_{RB41}K_{RO162} - K_{RB42}K_{RO161}) \quad (1)$$

$$C_{RO16} = (K_{RB41}d_{RO16} - K_{RB42}d_{RB4})/(K_{RB41}K_{RO162} - K_{RB42}K_{RO161}) \quad (2)$$

where C_{RB4} and C_{RO16} are RB4 and RO16 concentrations in binary mixtures, respectively; K_{RB41}, K_{RO161}, K_{RB42} and K_{RO162} are the RB4 and RO16 calibration constants at the two wavelengths 595 and 494 nm, respectively. The standard calibration curves were linear for RB4 and RO16 with $R^2 > 0.991$.

2.2. Sorption experiments

Different concentrations of working solution were prepared using stock solution (1000 mg/L reactive dyes in deionized water). With the aid of 0.1 M NaOH or HCl, the pH of dye solution was adjusted as well as maintained. The batch sorption experiments were conducted using 50 mL of reactive dye solution of desired concentration and known quantity of biochar in an Erlenmeyer flask (250 mL). For binary-dye systems, the concentration of two reactive dyes was maintained equally on weight basis. The suspension was agitated for 8 h using an incubated rotary shaker at 30 ± 1°C and 180 rpm. Once the sorption equilibrium was achieved, small amount of sample was pipetted and subse-

Table 1
Information of the reactive dyes

	Reactive blue 4	Reactive orange 16
Color index number	61205	17757
Molecular weight	637.43	617.54
Chemical formula	$C_{23}H_{14}Cl_2N_6O_8S_2$	$C_{20}H_{17}N_3Na_2O_{11}S_3$
Purity (%)	35	70
λ_{max} (nm)	595	494
Structure	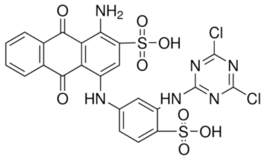	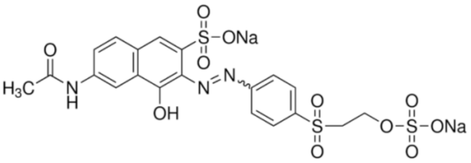

quently centrifuged (2100 rpm and 15 min). After centrifugation, the RB4/RO16 concentration in the supernatant solution was analysed using a spectrophotometer at respective wavelengths of two reactive dyes.

The amount of solute adsorbed by biochar can be calculated using the below relation:

$$U = V(C_i - C_e)/W \tag{3}$$

where U is the sorptional uptake (mmol/g); V is the solution volume (L); W is the biochar weight (g); C_i and C_e are the initial and equilibrium dye concentrations (mmol/L), respectively.

2.3. Analytical methods

The biochar surface was analysed using SEM (scanning electron microscopy). The sample was spread on copper grid then images were taken (Hitachi-S4800, Japan). Fourier transform infrared (FTIR) spectrum of biochar was recorded using Bruker-ATR IR (ACPHA, Germany) between 4000 and 600 cm^{-1} using KBr pellet procedure.

2.4. Single solute isotherm and kinetic modelling

Experimental RB4/RO16-biochar sorption isotherm were modelled using,

$$\text{Freundlich model: } U = K_F C_e^{1/n_F} \tag{4}$$

$$\text{Langmuir model: } U = \frac{U_{\max} b_L C_e}{1 + b_L C_e} \tag{5}$$

$$\text{Toth model: } U = \frac{U_{\max} b_T C_e}{[1 + (b_T C_e)^{1/n_T}]^{n_T}} \tag{6}$$

where K_F is the single solute Freundlich coefficient $(L/g)^{1/n_F}$, n_F is the Freundlich exponent, U_{max} is the single solute maximum reactive dye sorption capacity (mmol/g), b_L is the Langmuir equilibrium coefficient (L/mmol), b_T is the Toth model constant (L/mmol) and n_T is the Toth model exponent.

Experimental single solute dye-biochar sorption kinetics were modelled using,

$$\text{Pseudo 1}^{\text{st}}\text{order model } U_t = U_e(1 - \exp(-k_1 t)) \tag{7}$$

$$\text{Pseudo 2}^{\text{nd}}\text{order model } U_t = \frac{U_e^2 k_2 t}{1 + U_e k_2 t} \tag{8}$$

where U_e is the equilibrium reactive dye uptake (mmol/g), U_t is dye uptake at any time t (mmol/g), k_1 is the pseudo 1st order rate constant (1/min) and k_2 is the pseudo 2nd order rate constant (g/mmol·min).

The extended Langmuir equation, with a constant interaction factor was used to describe the binary adsorption isotherms of RB4-RO16 [20]:

$$U_{RB4} = \frac{U_{\max,RB4} b_{RB4} (C_{RB4}/\eta_{L,RB4})}{1 + b_{RB4}(C_{RB4}/\eta_{L,RB4}) + b_{RO16}(C_{RO16}/\eta_{L,RO16})} \tag{9}$$

$$U_{RO16} = \frac{U_{\max,RO16} b_{RO16} (C_{RO16}/\eta_{L,RO16})}{1 + b_{RB4}(C_{RB4}/\eta_{L,RB4}) + b_{RO16}(C_{RO16}/\eta_{L,RO16})} \tag{10}$$

where $U_{max,RB4}$, $U_{max,RO16}$, b_{RB4} and b_{RO16} are the mono component Langmuir parameters for RB4 and RO16, respectively. The interaction factors, $\eta_{L,RB4}$ and $\eta_{L,RO16}$ are for RB4 and RO16, respectively.

In addition, the multi-component Freundlich equation, Sheindrof-Rebhun-Sheintuch (SRS) equation [21] was used to represent RB4-RO16 binary isotherms,

$$(U)_i^j = K_{F_i} C_{e_i} [C_{e_i} + \theta_{ij} C_{e_j}]^{[(1/n_i)-1]} \tag{11}$$

where $(U)_i^j$ refers to dye uptake of solute (i) by biochar in the presence of competing solute (j), K_{Fi} is the mono-dye Freundlich constant for solute i, n_i is the single solute Freundlich exponent of solute i and θ_{ij} is the competitive coefficient.

The interaction factor was determined by reducing the below error function [15]:

$$\frac{100}{n-p} \sum_{i=1}^{n} \left[\frac{(U_{meas} - U_{cal})^2}{U_{meas}} \right]_i \tag{12}$$

where U_{cal} and U_{meas} are calculated and measured sorption capacities (mmol/g), respectively; n and p are the number of data points and parameters, respectively.

A non-linear regression procedure using the Sigma Plot (version 4.0, SPSS, USA) software was used to calculate the model parameters. The average percentage error between the predicted and experimental uptakes is determined through following equation:

$$\varepsilon(\%) = \frac{\sum_{i=1}^{N} (U_{\exp,i} - U_{cal,i}/U_{\exp,i})}{N} \times 100 \tag{13}$$

where U_{cal} and U_{exp} indicate the calculated and experimental dye uptakes (mmol/g), respectively, and N is the number of experimental data points. In the present study, all experiments were performed thrice and the results shown were the mean values of three different experimental trails.

3. Results and discussion

3.1. Surface examination of K. alvarezii-derived biochar

Fig. 1 illustrates SEM images of *K. alvarezii*-derived biochar (KAB) and dye-loaded KAB. The surface of KAB was found to be rough with varied pore sizes. This resulted in large specific surface area, which is a vital property of effective sorbent material. The cell wall of red marine algae majorly comprises of polysaccharides including agar and carrageenans [22,23]. These constituents offer negative binding sites including sulfonate and carboxylate for adsorption. The presence of these groups usually repels negatively charged reactive dye anions [24,25]. However, formation of more porous biochar from red seaweed is expected to perform better on sorption of anionic dyes through pore diffusion mechanism. It is also worth noting that surface of biochar tuned relatively smooth (Fig. 1) after

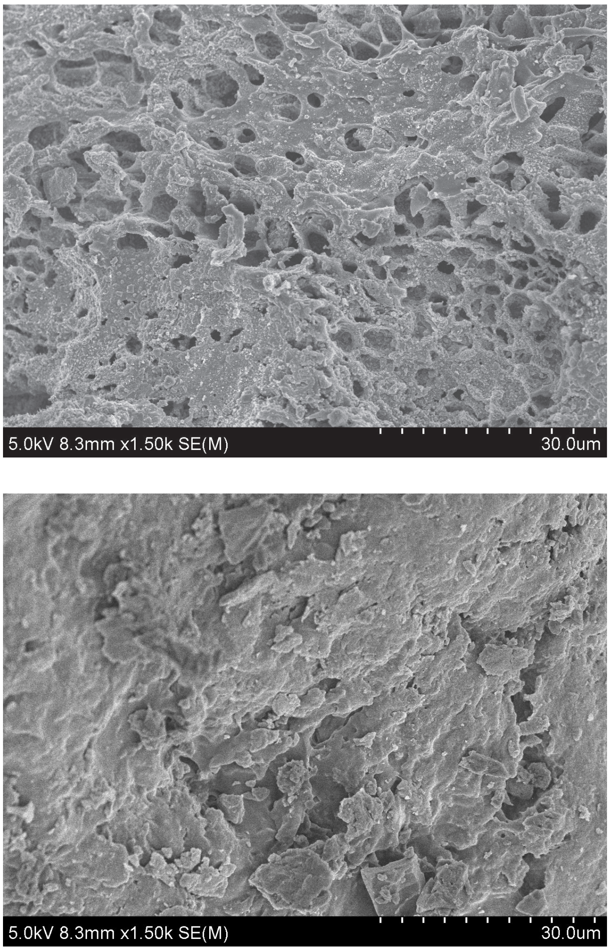

Fig. 1. Scanning electron micrographs of KAB and dye-loaded KAB.

dye sorption and this implies that impurities and other ions were released from seaweed surface due to strong acidic condition maintained during sorption experiments.

Fig. 2 shows the FTIR spectra of KAB. Analysis of FTIR spectra is vital to understand the characteristic binding sites of sorbents that involve in dye sorption. In the present study, the FTIR spectrum of KAB indicated the presence of strong bands at 1067 (C-O (alcohol) band), 1399 (symmetric C=O), 1619 (asymmetric C=O stretch of COOH), 2937 (C-H stretch) and 3421 (-NH, -OH stretching). Thus, it was clear that biochar exhibited a number of spectral peaks, thereby confirms the presence of wide variety of functional groups. The FTIR spectrum of RB4-RO16-loaded KAB showed significant variations in biochar functionalities after exposure to dye molecules (Fig. 2). The release of light metals (natural ions) from the biochar due to sorption of reactive dye molecules resulted in the above variation in FTIR result. The FTIR spectrum of RB4-RO16-loaded KAB indicated major shifts of bands at 1109 (C-O (alcohol) band), 1401 (symmetric C=O), 1615 (asymmetric C=O stretch of COOH), 2927 (C-H stretch) and 3427 (-NH, -OH stretching) (Fig. 2). The FTIR results further confirmed the possible participation of several binding sites on the biochar surface during electrostatic interaction of reactive dyes [26].

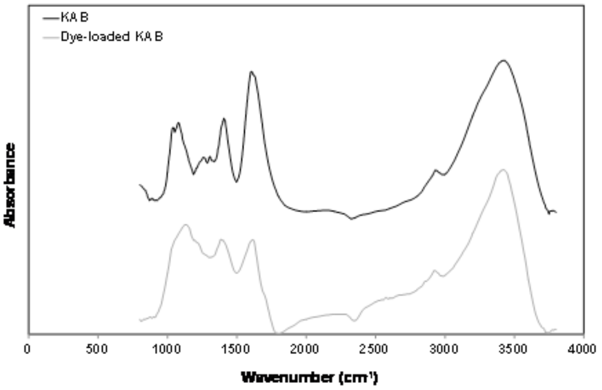

Fig. 2. Fourier transform infrared spectra of KAB and dye-loaded KAB.

3.2. Influence of pH

Initially, the effect of pH (equilibrium) on reactive dye adsorption was investigated through series of batch trials (Fig. 3). The dye equilibrium pH during sorption studies is important to assess the remediation capability of any adsorbent. Initial experiments were performed to compare the potential of KAB over raw *K. alvarezii* indicated that pyrolysis process improved the sorption capacity over 3.4 and 3.1 times for RB4 and RO16, respectively (Fig. 3). This confirms over previous assessment through SEM analysis that formation of more porous biochar resulted in increased sorption of anionic dyes through pore diffusion mechanism. During mono-dye solutions, sorption of RB4 and RO16 by KAB was high in strong acidic conditions (pH 2–4), about 50.3% and 21.0% decolorization was observed for RB4 and RO16, respectively at pH 3. As the pH was increased beyond 4, the sorption potential of KAB decreased as observed in Fig. 3. It is worth noting that KAB adsorbed more RB4 compared to RO16. The enhancement of reactive dye sorption in high acidic conditions (Fig. 3) is due to electrostatic interactions between the biochar and the reactive dye molecules [26,27]. Marine algae generally comprises of amine, carboxyl and sulfonate groups [28,29,30]. Therefore, in acidic conditions, it would be expected that the binding sites present on the biochar surface will be saturated with hydrogen ions (biochar protonation) and thereby biochar acquires total positive charge. On the other hand, RB4 and RO16 exist as Na^+ ions and $ROSO_3^-$ in solutions [13]. Thus, positively charged surface of the biochar attracts the negatively charged dye molecules through electrostatic attraction [31]. Thus, the mechanism of dye uptake by biochar can be considered as electrostatic interaction. In the process of adsorption, many factors influence the affinity as well as extent of sorption by the sorbent. This includes the characteristics of sorbent such as pore size distribution and specific surface area; as well as characteristics of dyes such as molar volume, molecular weight, shape, branching and flexibility [32]. Few researchers in the past correlated the extent of sorption with the size of dye molecules, with the assumption that smaller dye molecules tend to be sorbed better and faster [16,32]. The above assumption may be valid for the present study if the pores are small for RB4 and can accommodate only RO16. Then we can imply that competitive mechanism may

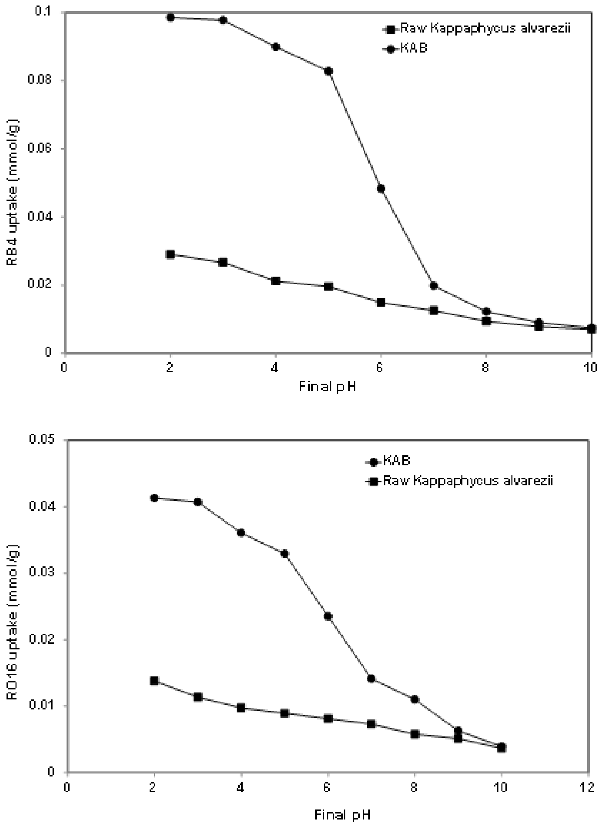

Fig. 3. Effect of equilibrium pH on sorption of RB4 and RO16 onto KAB in single solute systems (process conditions: initial dye concentration = 0.4 mmol/L; temperature = 30 ± 1°C).

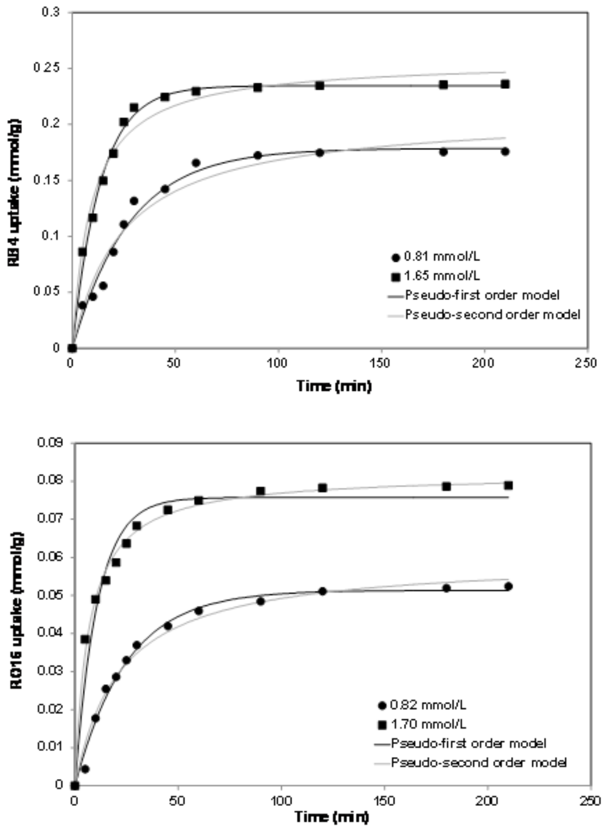

Fig. 4. Effect of contact time on sorption of RB4 and RO16 onto KAB in single solute systems. Curves were predicted by pseudo 1st and pseudo 2ndorder models (process conditions: pH = 3; temperature = 30 ± 1°C).

be pore blockage. However, the results (pH edge) implied that high molecular weight RB4 was favourably adsorbed over less molecular weight RO16 (Fig. 3). It should also be worth noting that the two reactive dyes used in the present study, RO16 and RB4 come under Remazol and Procion classes, respectively [13]. Fowler and Marshall [33] classified Remazol class dyes as moderately reactive, whereas Procion class as highly reactive. The result of the present study agrees with the above classification. During dyeing process, the reactivity of dye is crucial as it governs the dye diffusion rate into the fibre. In fact, dyes with high reactivity are preferential as it decrease the time required for batching process. It should also be pointed out that dye reactivity is controlled by solution pH, and the value usually increases with increase in pH [13]. At strong acidic conditions, RB4 is highly reactive; whereas RO16 require strong alkaline conditions to increase reactivity.

3.3. Kinetic studies of RB4 and RO16 onto KAB

The time course trials during sorption of RB4 and RO16 onto KAB from mono-solutions were performed to quantify the reaction time needed to achieve equilibrium. The results in Fig. 4 illustrate that process of sorption of RB4 and RO16 onto KAB was fast. Around 90% of total reactive dye sorption occurred within the first 60 min of contact. This rapid kinetics eventually slowed down after 60 min and the equilibrium was achieved after 180 min (Fig. 4). Due to excessive presence of strong functional groups during initial period, the concentration gradient between the dye molecules at the biochar surface and in the solution increases. This in turn increases fast sorption of reactive dyes onto KAB. However, as the time progresses, the strong functional groups were occupied and the low affinity functional groups contribute to limited sorption [34], which results in slow phase and eventual equilibrium attainment.

The pseudo 1st and 2nd order models were employed to understand the sorption kinetics of RB4 and RO16 onto KAB. Table 2 illustrates the model constants along with error values and correlation coefficients. In the present study, the modelling results indicated that the pseudo 1st order model slightly underestimated, whereas pseudo 2nd order kinetics overestimated the equilibrium experimental sorption capacities (U_e) values all concentration ranges examined. The pseudo 1st order model considers existence of external resistance or boundary layer at the start of adsorption; hence there exists a time lag in the model which leads to under predication of U_e values [35,36]. In general, slower kinetics are better described by the pseudo 1st order model. This aspect of underestimation as well as inability of the equation to describe whole range of kinetics data by pseudo 1st order model was observed in past studies [37,38]. On the other hand, the pseudo 2nd order model assumes

Table 2
The kinetics model constants obtained for removal of RB4 and RO16 by KAB

Model		RB4		RO16	
0.81 mmol/L		1.65 mmol/L	0.82 mmol/L	1.70 mmol/L	
Uptake estimated experimentally (mmol/g)		0.174	0.236	0.052	0.079
Pseudo 1st order	k_1 (min^{-1})	0.036	0.073	0.040	0.093
	U_e (mmol/g)	0.179	0.234	0.051	0.076
	% error	1.43	0.671	1.53	0.685
	R^2	0.981	0.994	0.990	0.965
Pseudo 2nd order	k_2 (g/(mmol.min))	0.192	0.416	0.777	1.82
	U_e (mmol/g)	0.210	0.258	0.060	0.082
	% error	3.74	1.05	3.81	0.698
	R^2	0.961	0.979	0.981	0.964

chemisorption as the rate controlling step and predicts the adsorption behaviour over entire range of dataset. Hence, pseudo 2nd order model better describes fast sorption kinetic process. As opposed to pseudo 1st order model, several researchers noted that pseudo 2nd order model tend to overestimate U_e values [39,40]. With the aid of % error and correlation coefficient values, the potential of two kinetic models to describe RB4 and RO16 experimental kinetics was also evaluated. The results indicated that both models exhibited reasonably high prediction with low % error and high correlation coefficient values (Table 2). Nevertheless, close analysis of statistical results indicated that the larger sized RB4 kinetics data was better described by pseudo 1st order model, whereas smaller sized RO16 kinetics data was better predicted pseudo 2nd order model. The experimental RB4 and RO16 kinetic data points along with curves as predicted by two models are presented in Fig. 4.

3.4. Isotherm

Experimental RB4 and RO16 sorption isotherms at pH 3 are plotted in Fig. 5. Sorption isotherms, a plot of sorption capacity (U) vs. equilibrium dye concentration (C_e) in the solution, are generally plotted to determine the full saturation capacity of any sorbent. In the present research, sorption isotherms were generated by changing the initial RB4/RO16 concentrations from 0.16–1.7 mmol/L at pH 3 (Fig. 5). For both reactive dyes, favourable concave shaped isotherms without strict plateau was observed. On comparing the isotherms, it was obvious that KAB displayed high RB4 sorption capacity. To be precise, the experimental RB4 uptake (0.236 mmol/g) was approximately 2.5 times higher than RO16 uptake (0.095 mmol/g).

The Langmuir, Freundlich and Toth models were employed to describe the single-component RB4/RO16 isotherm data. Considering these models comprise of constants that are easily interpretable as well as comparable to published literatures, they are preferred in this study. Of these models, the Langmuir model is one of the most widely used isotherm model that is useful to quantify maximum sorption capacities theoretically [41]. The values of U_{max} for RB4 and RO16 were calculated to be 0.324 and 0.140 mmol/g, respectively. The other Langmuir constant (b_L), which refers to affinity of reactive dyes towards KAB, was calculated to be 2.61 and 1.41 L/mmol for RB4 and RO16, respectively. This result clearly indicates KAB exhibited high affinity towards RB4 compared to RO16. Hence, more sorption of RB4 can be expected in binary solution. The %error values and correlation coefficients observed in the Langmuir model were between 0.73–1.13% and 0.989–0.998, respectively. Conversely, the application of the Freundlich model to the RB4/RO16 mono-dye isotherm data resulted in relatively low predication with high %error values and low correlation coefficients (Table 3). The binding capacity constant K_F values were determined to be 0.240 and 0.080 (mmol/g)(L/mmol)$^{1/n_F}$ for RB4 and RO16, respectively; whereas the Freundlich exponent was recorded as 2.14 and 1.91 for RB4 and RO16, respectively. Application of three parameter Toth model to the RB4/RO16 sorption isotherm data resulted in high prediction compared to two-parameter Langmuir and Freundlich models (Table 3). The Toth model is a three parameter equation that includes the features of both Langmuir and Freundlich equations. The model is based on the assumption of asymmetrical quasi-Guassian energy distribution with majority of binding groups possess sorption energy less than the mean or maximum values. Based on % error values and correlation coefficients, it was obvious that the Toth model performed well in predication of mono-dye RB4/RO16 isotherm data compared to the Langmuir

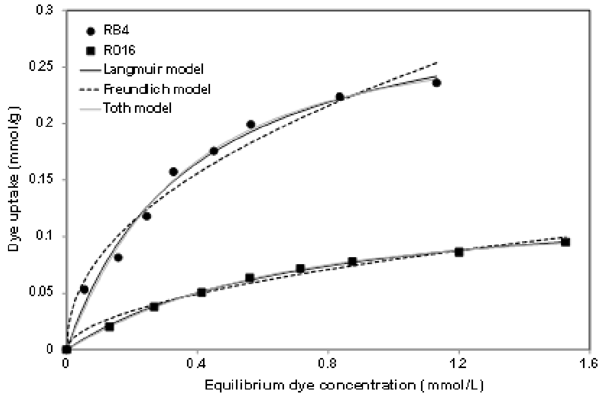

Fig. 5. Single solute sorption isotherms of RB4 and RO16 onto KAB. Curves were predicted by the Langmuir, Freundlich and Toth models (process conditions: pH = 3; temperature = 30 ± 1°C).

Table 3
Isotherm model constants obtained during sorption of RB4 and RO16 from single and dual component systems

Model		RB4	RO16
Langmuir	b_L (L/mmol)	2.61	1.41
	U_{max} (mmol/g)	0.324	0.140
	% error	1.13	0.73
	R^2	0.989	0.998
Freundlich	K_F (mmol/g) (L/mmol)$^{1/n_F}$	0.240	0.080
	n	2.14	1.91
	% error	3.07	1.48
	R^2	0.973	0.982
Toth	b_T (L/mmol)	2.47	1.42
	U_{max} (mmol/g)	0.285	0.116
	n_T	0.761	0.716
	% error	1.11	0.42
	R^2	0.990	0.999
Extended Langmuir	$\eta_{L,1}$	1.3	–
	$\eta_{L,2}$	–	2.45
	% error	1.97	5.30
	R^2	0.995	0.996
SRS equation	θ_1	0.49	–
	θ_2	–	12.2
	% error	9.47	0.36
	R^2	0.977	0.994

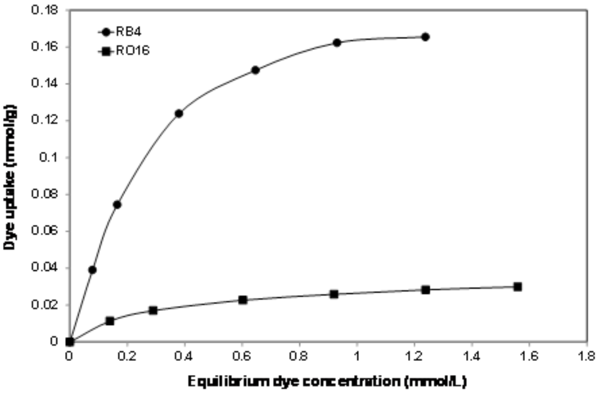

Fig. 6. Experimental sorption isotherms of RB4 and RO16 in binary mixtures onto KAB (process conditions: pH = 3; temperature = 30 ± 1°C).

and Freundlich models. Fig. 5 illustrates the RB4/RO16 isotherm experimental points and predicted curves of all three models.

As seen in binary sorption isotherm curves, the KAB accommodated more RB4 compared to RO16 (Fig. 6). Even though slightly lower than pure RB4 system, KAB sorbed more RB4 molecules in the presence of RO16. On the other hand, RO16 uptake was severely supressed by RB4 in comparison to its mono-dye isotherm data. From the binary isotherm (Fig. 6), the highest RB4 and RO16 experimental uptakes were estimated to be 0.166 and 0.030 mmol/g, respectively. This indicates that RB4 uptake was 5.5 times than that of RO16. This value was 2.5 times in mono-component RB4-RO16 system. Thus the results pointed out the high affinity of RB4 towards KAB as well as strong binding inhibition of RO16 onto KAB. The reason for high RB4 sorption by KAB was discussed in Section 3.2.

To describe binary-dye isotherm, we have used an extended Langmuir model coupled with constant interaction factor. Considering that traditional multi-solute Langmuir equation assumes zero interaction among sorbates, identical competition between sorbates to occupy binding sites as well as constant energy of sorption, it may not be valid for real effluents [15]. In order to include interaction as well as competition among sorbates, an interaction factor (η) has been added to the original equation [20] and has the form as shown in Eqs. (9) and (10). For the current investigation, η is specific to each dye and also have a constant value in the binary-dye system. Using error-minimization technique, η values were determined to be 1.3 and 2.45 for RB4 and RO16, respectively. High value of interaction factor observed for RO16 confirmed high competition of RB4 over RO16. The model also performed well in prediction of RB4/RO16 binary-isotherm with high low % error and high correlation coefficient values (Table 3). Although, the extended Langmuir model uses corresponding mono-dye isotherm model parameters to describe binary-dye isotherms, it effectively predicted the interaction and competition between RB4 and RO16 in binary solutions. As a next attempt in multi-component modelling, a multi-component Freundlich equation (SRS equation) with competitive coefficient (θ_{ij}) was used. The model based on the assumption that each solute comprises of exponential distribution of adsorption energies. Application of SRS equation to binary RB4/RO16 isotherm resulted in good prediction with low % error values and high correlation coefficients (Table 3). Similar to the experimental results, the model predicted high RB4 competition over RO16 as high competitive coefficient was observed for RO16 (12.2) over RB4 (0.49). Even though empirical models reasonably described the multi-dye biosorption isotherm, it should be emphasized that mechanistic models, based on a series of physico-chemical reactions [42] would allow more insight of competitive sorption process. Fig. 7 presents 3D plot of binary-RB4/RO16 isotherm experimental data as well as curves predicted by two examined models.

4. Conclusions

Wastewaters discharged from several dye-based industries are cause of concern owing to the presence of several dye components. However, most of the previous studies focus on single-dye systems and recommend sorbent based on the results. However, through this study, we recommend that sorption techniques should consider competition and interaction between dyes present in the wastewaters, prior to process recommendation. Thus in this study, the competition incurred by RB4 and RO16 during sorption onto *K. alvarezii*-derived biochar was evaluated. Single-solute systems clearly indicated that KAB showed high preference towards RB4 over RO16. However,the presence of RB4 and RO16 in binary solutions resulted in strong competition

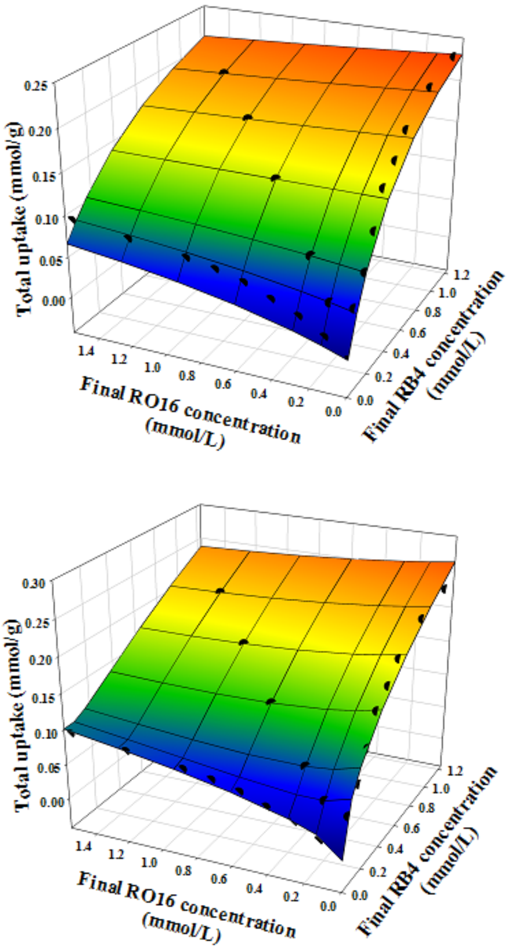

Fig. 7. Total dye uptake as the function of final (equilibrium) concentration in the RB4-RO16 dual sorption system. Mesh surface predicted by the extended Langmuir model (top image) and extended Freundlich SRS equation (bottom image). Experimental results are shown by discrete points.

resulted in decrease in overall uptake. The single component isotherm data were modelled successfully using the three-parameter Toth model, whereas complex multi-dye isotherms were described successfully using the SRS equation and competitive Langmuir model with constant interaction factor. Thus the present study has indicated the importance to study multi-component sorption systems to design wastewater scheme for real dye effluents.

References

[1] Z. Aksu, Application of biosorption for the removal of organic pollutants: a review, Proc. Biochem., 40 (2005) 997–1026.

[2] Z. Aksu, S.S. Çağatay, Investigation of biosorption of Gemazol Turquoise blue-G reactive dye by dried Rhizopus arrhizus in batch and continuous systems, Sep. Purif. Technol., 48 (2006) 24–35.

[3] J. Pierce, Colour in textile effluents-the origins of the problem, J. Soc. Dyers Colourists, 110 (1994) 131–134.

[4] Y.M. Slokar, A.M. Le Marechal, Methods of decolorization of textile wastewaters, Dyes Pigments, 37 (1998) 335–356.

[5] K. Vijayaraghavan, M.W. Lee, Y.-S. Yun, A new approach to study the decolorization of complex reactive dye bath effluent by biosorption technique, Biores. Technol., 99 (2008) 5778–5785.

[6] M.M. Hassan, C.M. Carr, A critical review on recent advancements of the removal of reactive dyes from dyehouse effluent by ion-exchange adsorbents, Chemosphere, 209 (2018) 201–219.

[7] H. Chaudhuri, S. Dash, A. Sarkar, Fabrication of new synthetic routes for functionalized si-mcm-41 materials as effective adsorbents for water remediation, Ind. Eng. Chem. Res., 55 (2016) 10084–10094.

[8] H. Chaudhuri, S. Dash, R. Gupta, D.D. Pathak, A. Sarkar, Room-temperature in-situ design and use of graphene oxide-sba-16 composite for water remediation and reusable heterogeneous catalysis, Chem. Select, 2 (2017) 1835–1842.

[9] V.K. Gupta, Suhas, Application of low-cost adsorbents for dye removal-a review, J. Environ. Manage., 90 (2009) 2313–2342.

[10] H. Chaudhuri, S. Dash, A. Sarkar, SBA-15 functionalised with high loading of amino or carboxylate groups as selective adsorbent for enhanced removal of toxic dyes from aqueous solution, New J. Chem., 40 (2016) 3622–3634.

[11] H. Chaudhuri, S. Dash, A. Sarkar, Single-step room-temperature in situ syntheses of sulfonic acid functionalized sba-16 with ordered large pores: potential applications in dye adsorption and heterogeneous catalysis. Ind. Eng. Chem. Res., 56 (2017) 2943–2957.

[12] L.P. Mazur, M.A.P. Cechinel, S.M.A.G.U. de Souza, R.A.R. Boaventura, V.J.P. Vilar, Brown marine macroalgae as natural cation exchangers for toxic metal removal from industrial wastewaters: A review, J. Environ. Manage., 223 (2018) 215–253.

[13] K. Vijayaraghavan, Y.-S. Yun, Competition of Reactive red 4, Reactive orange 16 and Basic blue 3 during biosorption of Reactive blue 4 by polysulfone-immobilized *Corynebacterium glutamicum*, J. Hazard. Mater., 153 (2008) 478–486.

[14] A.R.A. Giwa, K.A. Abdulsalam, M.A. Oladipo, A.O. Ibrahim, Adsorption of crystal violet from quaternary dye mixture onto sawdust: statistical analysis and optimization studies, J. Environ. Biotechnol. Res., 7(4) (2018) 54–63.

[15] K.K.H. Choy, J.F. Porter, G. McKay, Langmuir isotherm models applied to the multicomponent sorption of acid dyes from effluent onto activated carbon, J. Chem. Eng. Data, 45 (2000) 575–585.

[16] M.-S. Chiou, G.-S. Chuang, Competitive adsorption of dye metanil yellow and RB15 in acid solutions on chemically cross-linked chitosan beads, Chemosphere, 62 (2006) 731–740.

[17] K. Vijayaraghavan, K. Palanivelu, M. Velan, Crab shell-based biosorption technology for the treatment of nickel-bearing electroplating industrial effluents, J. Hazard. Mater., 119 (2005) 251–254.

[18] Z. Mahdi, A. El Hanandeh, Q. Yu, Influence of pyrolysis conditions on surface characteristics and methylene blue adsorption of biochar derived from date seed biomass, Waste Biomass Valorization, 8 (2017) 2061–2073.

[19] B. Al-Duri, G. McKay, Prediction of binary systems of batch adsorption using basic dyes onto activated carbon, Chem. Eng. Sci., 46 (1991) 193–204.

[20] G. McKay, B. Al-Duri, Simplified model for the equilibrium adsorption of dyes from mixtures using activated carbon, Chem. Eng. Proc., 22 (1987) 145–156.

[21] C. Sheindrof, M. Rebhun, M. Sheintuch, A Freundlich type multicomponent isotherm, J. Coll. Interf. Sci., 79 (1981) 136–142.

[22] R.S. Praveen, K. Vijayaraghavan, Optimization of Cu (II), Ni (II), Cd (II) and Pb (II) biosorption by red marine alga *Kappaphycusalvarezii*, Desal. Water Treat., 55 (2015) 1816–1824.

[23] D. Krishnaiah, D.M.R. Prasad, A. Bono, P.M. Pandiyan, R. Sarbatly, Application of ultrasonic waves coupled with functional link neural network for estimation of carrageenan concentration, Int. J. Phys. Sci., 3 (2008) 90–96.

[24] K. Vijayaraghavan, M. Sathishkumar, R. Balasubramanian, Interaction of rare earth elements with a brown marine alga in multi-component solutions, Desalination, 265 (2011) 54–59.

[25] H.R. Ong, D.M.R. Prasad, M.R. Khan, D.S. Rao, J. Nitthiyah, D.K. Raman, Effect of Jatropha seed oil meal and rubber seed oil meal as melamine urea formaldehyde adhesive extender on the bonding strength of plywood, J. Appl. Sci., 12 (2012) 1148–1153.

[26] O.D. Nartey, B. Zhao, Biochar preparation, characterization, and adsorptive capacity and its effect bioavailability of contaminants: an overview, Adv. Materials Sci. Eng., vol. 2014 (2014) Article ID 715398, 12 pages.

[27] H. Li, X. Dong, E.B. da Silva, L.M. de Oliveira, Y. Chen, L.Q. Ma, Mechanisms of metal sorption by biochars: Biochar characteristics and modifications, Chemosphere, 178 (2017) 466–478.

[28] T.A. Davis B. Volesky A. Mucci, A review of the biochemistry of heavy metal biosorption by brown algae, Water Res., 37 (2003) 4311– 4330.

[29] R. Senthilkumar, D.D.A. Aljoubory R, Phenol degradation of industrial wastewater by photocatalysis, J. Innovative Eng., 2(2) (2014) 5.

[30] R. Senthilkumar D.M.R. Prasad L. Govindarajan K. Saravanakumar, B.S.N. Prasad, Green alga-mediated treatment process for removal of zinc from synthetic solution and industrial effluent, Environ. Technol., (2017) in press. doi: 10.1080/09593330.2017.1420696.

[31] V. Janaki, K. Vijayaraghavan, A.K. Ramasamy, K.J. Lee, B.T. Oh, S. Kamala-Kannan, Competitive adsorption of Reactive Orange 16 and Reactive Brilliant Blue R on polyaniline/bacterial extracellular polysaccharides composite - A novel ecofriendly polymer, J. Hazard. Mater., 241 (2012) 110–117.

[32] H. Mètivier-Pignon, C. Faur-Brasquet, P. Le Cloirec, Adsorption of dyes onto activated carbon cloths: approach of adsorption mechanisms and coupling of ACC with ultrafiltration to treat coloured wastewaters, Sep. Purif. Technol., 31 (2003) 3–11.

[33] J.A. Fowler, W.J. Marshall, Reactive dyes: the technical basis for choosing between dyes of high and dyes of low reactivity, J. Soc. Dyers Colourists, 80 (1964) 358–363.

[34] O.S. Ayanda, D. Malomo, K.O. Sodeinde, O.O. Oketayo, O.N. Abdulazeez, Isotherm, kinetics, and thermodynamics of arsenic (III) adsorption onto activated carbon, J. Environ. Biotechnol. Res., 6(1) (2017) 179–185.

[35] G. McKay, Y.S. Ho, J.C.Y. Ng, Biosorption of copper from wastewaters: a review, Sep. Purif. Meth., 28 (1999) 87–125.

[36] S. Ramalingam, L. Parthiban, P. Rangasamy, Biosorption modeling with multilayer perceptron for removal of lead and zinc ions using crab shell particles, Arabian J. Sci. Eng., 39 (2014) 8465–8475.

[37] Z. Reddad, C. Gerente, Y. Andres, P.L. Cloirec, Adsorption of several metal ions onto a low-cost biosorbent: Kinetic and equilibrium studies, Environ. Sci. Technol., 36 (2002) 2067–2073.

[38] M. Sathishkumar, A. Mahadevan, K. Vijayaraghavan, S. Pavagadhi, R. Balasubramanian, Green recovery of gold through biosorption, biocrystallization, and pyro-crystallization, Ind. Eng. Chem. Res., 49 (2010) 7129–7135.

[39] A.E. Ofomaja, E.B. Naidoo, S.J. Modise, Dynamic studies and pseudo-second ordermodeling of copper(II) biosorption onto pine cone powder, Desalination, 251 (2010) 112–122.

[40] M. Sathishkumar, S. Pavagadhi, K. Vijayaraghavan, R. Balasubramanian, Experimental studies on removal of microcystin-LR by peat, J. Hazard. Mater., 184 (2010) 417–424.

[41] M. Sathishkumar, A.R. Binupriya, K. Vijayaraghavan, S.I. Yun, Two and three-parameter isothermal modeling for liquid-phase sorption of Procion Blue H-B by inactive mycelial biomass of *Panusfulvus*, J. Chem. Technol. Biotechnol., 82 (2007) 389–398.

[42] F. Pagnanelli, A. Esposito, F. Vegliò, Multi-metallic modeling for biosorption of binary systems, Water Res., 36 (2002) 4095–4105.